JOURNAL OF SPACECRAFT AND ROCKETS
Vol. 31, No. 2, March–April 1994

Calculations of Low-Reynolds-Number Resistojet Nozzles

Suk C. Kim*
Sverdrup Technology, Inc., Brook Park, Ohio 44142

Calculations are made for low-Reynolds-number resistojet nozzles using a full Navier-Stokes code. To study the effects of viscous and divergence losses on performance, flowfields and specific impulses of hydrogen resistojet nozzles with various lengths and shapes, such as 20-deg, 30-deg half-angle conical nozzles and a contoured nozzle, are calculated and compared with each other. The calculated results for these nozzles with a throat Reynolds number of 1150 are presented as Mach-number contours, centerline variations of Mach number and static temperature, exit profiles of Mach number and axial velocity, and axial variations of vacuum specific impulse. The present calculations show that the vacuum specific impulse of the 30-deg half-angle conical nozzle is the highest among those of the three nozzles. Calculations are also made for a nozzle with a throat Reynolds number of 270 to validate the code and the results agree reasonably well with the experimental data.

Nomenclature

e	= total internal energy
F, G	= inviscid fluxes
F_v, G_v	= viscous fluxes
H	= source term
I_{sp}	= specific impulse [see Eq. (3)]
k	= thermal conductivity
$\dot{m}$	= mass flow rate, kg/s
p	= pressure, Pa
q	= heat flux
Re_t	= throat Reynolds number [see Eq. (2)]
r_t	= throat radius
T	= temperature, K
t	= time
u	= axial velocity, m/s
v	= radial velocity, m/s
x, r, θ	= cylindrical coordinates
μ	= laminar viscosity
ρ	= density, kg/m^3
τ	= shear stress
σ	= normal stress

Subscripts

c	= centerline
e	= exit
o	= stagnation or chamber
t	= throat
w	= wall

Introduction

ELECTROTHERMAL thrusters, such as arcjets and resistojets, have potential for high performance. In particular, resistojets can be used on geostationary satellites for attitude control and north-south stationkeeping which require a thrust less than 0.4 N. To generate such low thrusts, resistojets are designed to operate at low chamber pressures and have small nozzle dimensions. These restrictions result in low Reynolds numbers of the flows, therefore, the viscous losses are significant in these thruster nozzles. In designing a nozzle with a given area ratio, the reduction of the nozzle length can decrease the viscous loss but increase the divergence loss due to the increase in the exit angle of the nozzle; thus, there are two competing losses, viscous loss and divergence loss.

In the past, study of low-Reynolds-number flow has been made for supersonic nozzles,[1,2] nozzles for chemical laser,[3–5] low-density hypersonic nozzles,[6,7] and nozzles with various contours.[8–11] It was found in these studies that the viscous layer inside the nozzle becomes thicker as the Reynolds number decreases and the flow inside the nozzle becomes fully viscous at very low Reynolds number. It was also found in these studies that bell-shaped nozzles tend to be lower in efficiency than 20-deg and 25-deg half-angle conical nozzles at low Reynolds numbers. An excellent summary of previous studies can be found in Ref. 11. An experimental study made previously on the performance of 15-deg, 20-deg, and 25-deg half-angle conical nozzles, bell nozzles, and trumpet nozzles showed that the trumpet and 25-deg half-angle conical nozzles perform slightly better than the other nozzles, but it was unclear which is superior as all fell within the experimental error band.[11] The recent experimental results for performance and endurance of multipropellant resistojets for an auxiliary propulsion system of the space station can be found in Refs. 12 and 13.

In designing a rocket nozzle for a given area ratio, the Rao nozzle optimization code,[14] which is based on the inviscid flow assumption, is widely used to obtain the optimum nozzle wall contour. But the bell-shaped nozzle whose wall contour is obtained from the Rao code may not give the highest specific impulse at low-Reynolds-number flow conditions because the Rao code uses the methods of characteristics (MOC), neglecting the viscous loss which is significant at low Reynolds number. Thus, accurate performance prediction of low-Reynolds-number resistojet nozzles with various shapes and lengths is needed to select the length and shape of the nozzle which gives the highest performance value for a given area ratio.

For performance prediction of rocket nozzles, the Joint Army, Navy, NASA, Air Force (JANNAF) two-dimensional kinetics code with a boundary-layer module (TDK/BLM) has been commonly used. But it has difficulties in predicting the performance of low-Reynolds-number nozzles because it solves the flowfields by the methods of characteristics with a boundary-layer correction.[15] For the calculations of low-Reynolds-number nozzle flows, some investigators have used the Rae code,[2] which is based on the slender-channel approximation of the Navier-Stokes equations, but it has limitations due to the use of the boundary-layer assumptions.

In the present study, a full Navier-Stokes code, the RPLUS code, is used to calculate the flowfields of low-Reynolds-number nozzles. The code, which was developed at NASA Lewis Research Center,[16] employs an implicit finite volume, LU-SSOR scheme to solve the full Navier-Stokes equations and the species equations in a coupled manner, and has been previously used to calculate H_2/O_2 thruster flowfields,[17,18] high-area-ratio H_2/O_2 orbital transfer vehicle performance,[19] and nuclear thermal rocket flowfields.[20,21]

To study the two competing losses, the viscous loss and the divergence loss, the flowfields and performance values of hydrogen resistojet nozzles with various lengths and shapes, such as 20-deg, 30-deg half-angle conical nozzles and a contoured nozzle

Received Nov. 9, 1992; revision received Feb. 22, 1993; accepted for publication Feb. 22, 1993.

*Senior Research Engineer, Lewis Research Center Group, 2001 Aerospace Parkway. Member AIAA.

whose wall contour is obtained from the Rao code, are calculated and compared with each other. These nozzles have an area ratio of 82 and will be called the resistojet nozzles. For the validation of the present code, flowfields of a very low-Reynolds-number nozzle are calculated and compared with the experimental data obtained by an electron-beam technique.[1] This nozzle has an area ratio of 66 and will be called the Rothe nozzle.

Numerical Method

The Navier-Stokes equations for axisymmetric laminar flow can be written as follows:

$$\frac{\partial Q}{\partial t} + \frac{\partial (F - Fv)}{\partial x} + \frac{1}{r}\frac{\partial [r(G - G_v)]}{\partial r} = H \tag{1}$$

$$Q = \begin{pmatrix} \rho \\ \rho u \\ \rho v \\ \rho e \end{pmatrix}, \quad F = \begin{pmatrix} \rho u \\ \rho u^2 + p \\ \rho uv \\ u(\rho e + p) \end{pmatrix}$$

$$F_v = \begin{pmatrix} 0 \\ \sigma_{xx} \\ \tau_{rx} \\ u\sigma_{xx} + v\tau_{xr} - q_x \end{pmatrix}, \quad G = \begin{pmatrix} \rho v \\ \rho uv \\ \rho v^2 + p \\ v(\rho e + p) \end{pmatrix}$$

$$G_v = \begin{pmatrix} 0 \\ \tau_{rx} \\ \sigma_{rr} \\ v\sigma_{rr} + u\tau_{xr} - q_r \end{pmatrix}, \quad H = \begin{pmatrix} 0 \\ 0 \\ -\tau_{\theta\theta}/r \\ 0 \end{pmatrix}$$

where

$$\sigma_{xx} = 2\mu u_x - \frac{2}{3}\mu\left(u_x + v_r + \frac{v}{r}\right)$$

$$\sigma_{rr} = 2\mu v_r - \frac{2}{3}\mu\left(u_x + v_r + \frac{v}{r}\right)$$

$$\tau_{xr} = \tau_{rx} = \mu(u_r + v_x)$$

$$\tau_{\theta\theta} = \frac{4}{3}\mu\frac{v}{r} - \frac{2}{3}\mu(u_x + v_r) - p$$

$$q_x = -kT_x$$

$$q_r = -kT_r$$

In the RPLUS code, the lower-upper symmetric successive overrelaxation (LU-SSOR) scheme[22] is used to solve the above equations. The LU-SSOR scheme employs an implicit Newton iteration technique to solve the finite volume approximation of the steady-state version of the governing equations. Detailed description of the LU-SSOR scheme can be found in Refs. 16 and 22. In the code, the specific heat, thermal conductivity, and viscosity are given as fourth-order polynomials of temperature and the coefficients of these polynomials are valid up to a temperature of 6000 K.

Nozzle Geometry

Resistojet Nozzles

The hydrogen resistojet nozzles calculated in the present study are 20-deg and 30-deg half-angle conical nozzles and a contoured nozzle whose wall contour is obtained from the Rao code. The area ratio of the nozzles is 82 and the throat radius is 0.42 mm. These nozzles have a thrust level of 0.12 N and their throat Reynolds numbers are 1150 for the chamber temperature of 1500 K and the chamber pressure of 0.15 MPa. The throat Reynolds number Re_t is defined as

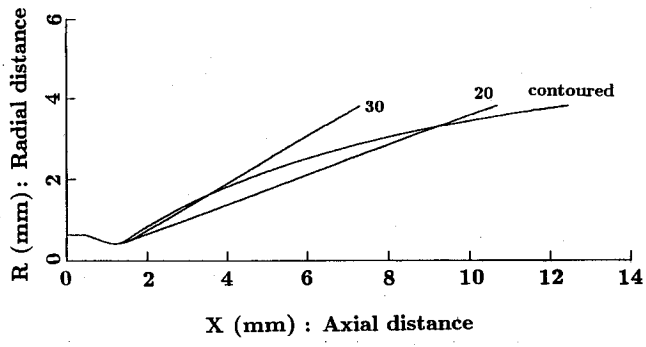

Fig. 1 Wall contours of various resistojet nozzles.

$$Re_t = 2\dot{m}/\pi\mu_o r_t \tag{2}$$

The radii of curvature upstream and downstream of the throat are 1.5 times the throat radius and the area ratio at the inlet is 2.25.

Figure 1 shows the wall contours of various hydrogen resistojet nozzles. As shown in this figure, the throat and exit radii of the three nozzles are all the same, but the nozzle lengths and wall contours are different from each other. The throat is located at $x = 1.23$ mm, and the total length of the nozzle ranges from about 7.2 mm for the 30-deg half-angle conical nozzle to 12.3 mm for the contoured nozzle. Immediately downstream of the throat, the expansion of the contoured nozzle is the most rapid of the three nozzles; then, its expansion angle decreases to 7.85 deg at the exit.

Rothe Nozzle

The Rothe nozzle is a very low-Reynolds-number nozzle with an area ratio of 66 and it uses nitrogen as a propellant. It is a 20-deg half-angle conical nozzle and its length and throat radius are 56 and 2.55 mm, respectively. The radii of curvature upstream and downstream of the throat are the throat radius, and the area ratio at the inlet is 2.25. The throat Reynolds number for the chamber temperature of 300 K and the chamber pressure of 474 Pa is 270. The experimental data for the Rothe nozzle are available and they were obtained by an electron-beam technique.[1] In the experiment, the density and rotational temperature were measured and the ambient pressure was 1.5 Pa.

Boundary Conditions

In the present study, it is assumed that the inflow total enthalpy and total pressure are constant at the nozzle inlet where the area ratio is 2.25. The inlet radial velocity is assumed to be zero and the inlet axial velocity is obtained by extrapolation from the interior; then, the static temperature at the inlet is obtained from the inflow total enthalpy and the inlet axial velocity, and the static pressure and density at the inlet are obtained from the isentropic relation and the equation of state, respectively.

At the exit of the nozzle where the large portion of the flow is supersonic, all dependent variables are extrapolated from the interior. For the low-Reynolds-number nozzle, some portion of the exit flow near the nozzle wall is subsonic. In the subsonic region at the exit, the static pressure should be specified as a boundary condition but it is unknown for the nozzle operating in space where the ambient pressure is near zero and the flow expands around the nozzle lip and into the region upstream of the nozzle exit plane. Thus in the present study, the extrapolation is also used in the subsonic region at the exit. Fortunately, the effect of ambient pressure on the vacuum specific impulse of low-Reynolds-number nozzle is found to be very small as long as the ambient pressure is sufficiently low that the flow does not separate and a shock wave does not exist in the nozzle.[23,24]

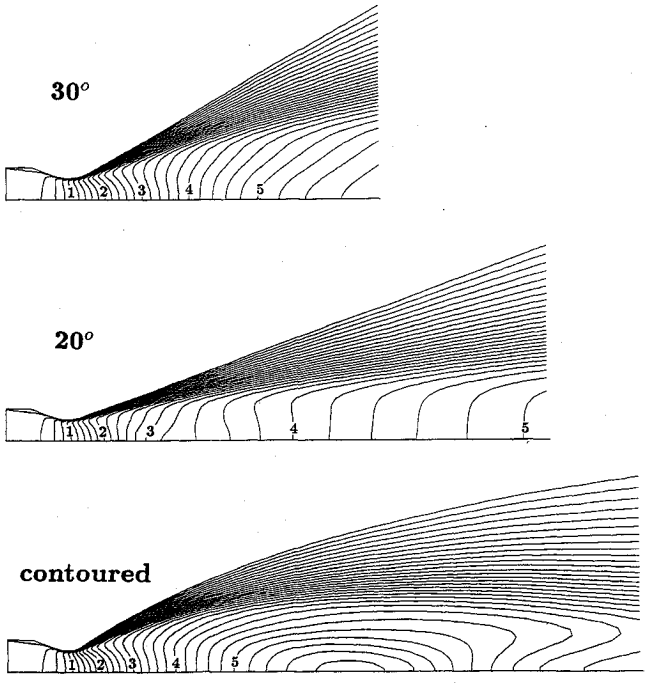

Fig. 2 Mach-number contours for various resistojet nozzles.

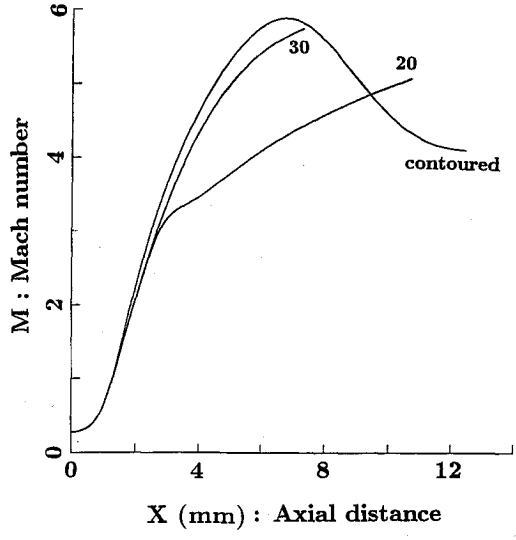

Fig. 3 Axial variations of centerline Mach number.

For the present nozzles, the Knudsen number, which is defined as the ratio of the mean free path to the characteristic length, is relatively high near the exit; thus, the flow is near-rarefied and there can be a velocity slip at the nozzle wall. In the present study, however, the no-slip condition is used at the wall, and the wall is assumed to be adiabatic. At the axis of symmetry, the radial velocity and the radial derivatives of the other dependent variables are set to be zero.

Results and Discussion

The calculations are made with a 240×60 grid. A very small uniform axial grid size is used from the inlet to some distance downstream of the throat, after which the grid spacing increases. The radial grid size becomes finer near the wall.

Resistojet Nozzles

Calculations are made for the chamber temperature of 1500 K and the chamber pressure of 0.15 MPa. The throat Reynolds number of the resistojet nozzles at these chamber conditions is 1150 and hydrogen is used as a propellant. To check the global conservation of the present solutions, the mass fluxes at all axial stations are calculated and compared with the inflow mass flux. The results show that the overall error in mass conservation is never more than ± 0.28%, which is adequate for most engineering estimates. The mass flux errors at the exits of the 20-deg and 30-deg half-angle conical nozzles are less than 0.042%, whereas that of the contoured nozzle is 0.132%.

Figure 2 shows the Mach-number contours for various resistojet nozzles from the present calculations. As seen from Fig. 2, the subsonic inflow rapidly accelerates through the converging-diverging nozzle to become supersonic and the viscous layers along the nozzle walls are very thick. Because of the smaller viscous loss due to the shorter length of the 30-deg half-angle conical nozzle, the viscous layer of the 30-deg half-angle conical nozzle at the exit is thinner than those of the other two nozzles. Due to the significant viscous effect, about 70% of the exit radius is the viscous layer for the contoured nozzle, which is the longest among the three nozzles. Because of the rapid expansion just after the throat and subsequent gradual expansion, compression waves are formed near the

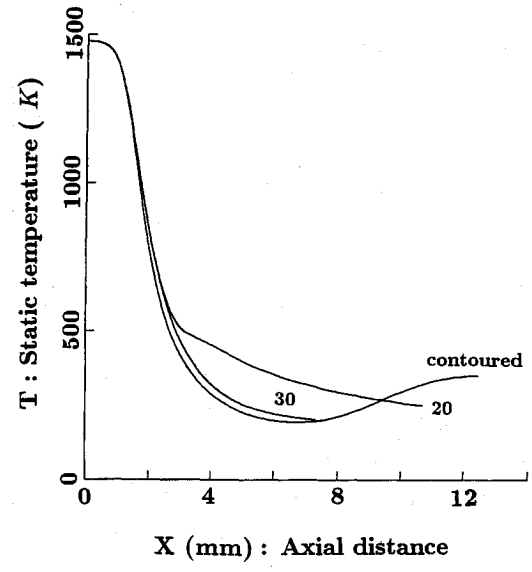

Fig. 4 Axial variations of centerline static temperature.

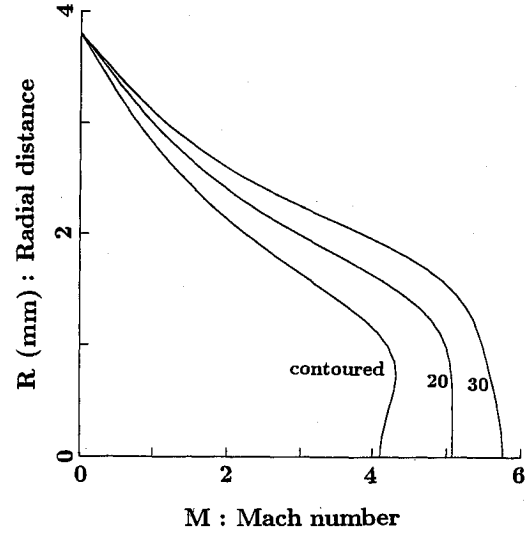

Fig. 5 Exit Mach-number profiles.

inflection point of the diverging section of the contoured nozzle and strike the centerline, as seen from Fig. 2.

Figures 3 and 4 show the Mach number and static temperature variations along the centerlines of the various nozzles. As seen from Fig. 3, the centerline Mach numbers of the 20-deg and 30-deg half-angle conical nozzles increase through the converging-diverging nozzles, while that of the contoured nozzle increases until x = 6.5 mm and then decreases due to the presence of the compression waves. The centerline Mach number of the contoured nozzle near the nozzle throat is the largest among those of the three nozzles due to the more rapid expansion of the contoured nozzle after the nozzle throat than those of the two conical nozzles. At the exits of the nozzles, the centerline Mach number of the 30-deg half-angle conical nozzle is 5.8, while those of the 20-deg half-angle conical and contoured nozzles are 5.1 and 4.1, respectively. The static temperature variations along the centerline show the same trends as those of the Mach number as seen from Fig. 4.

Figure 5 shows the Mach-number profiles at the exits of the various resistojet nozzles. As seen in this figure, the nozzle wall viscous layers are very thick and the exit Mach number of the 30-deg half-angle conical nozzle is the largest whereas that of the contoured nozzles is the smallest among those of the three nozzles. The exit static temperature profiles show the same trends as those of the Mach number as seen from Fig. 6. Figure 7 shows the axial velocity profiles at the exits of various resistojet nozzles. The exit axial velocity of the 30-deg half-angle conical nozzles is the largest whereas that of the contoured nozzle is the smallest as seen from this figure. Figure 8 shows the radial velocity profiles at the exits of the various resistojet nozzles. The magnitude of the exit radial velocity, the divergence loss, is the largest for the 30-deg half-angle conical nozzle because the exit angle of the 30-deg half-angle conical nozzle is larger than those of the other two nozzles. Because of the presence of the compression waves, the exit radial velocity near the centerline of the contoured nozzle is negative as seen from Fig. 8.

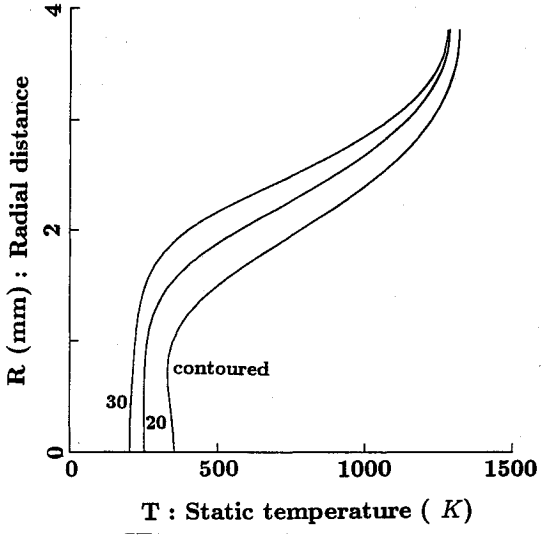

Fig. 6 Exit static temperature profiles.

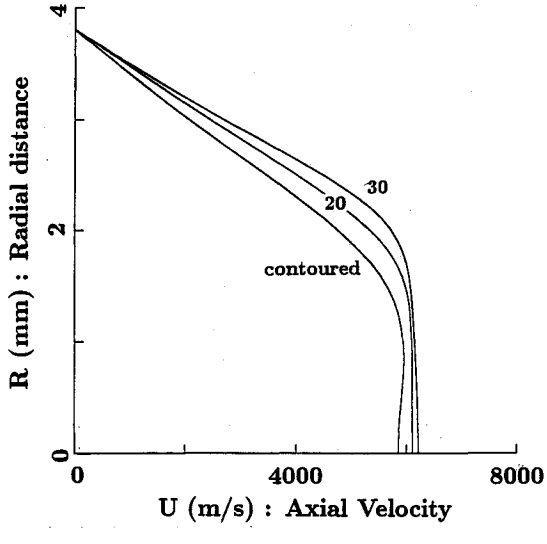

Fig. 7 Exit axial velocity profiles.

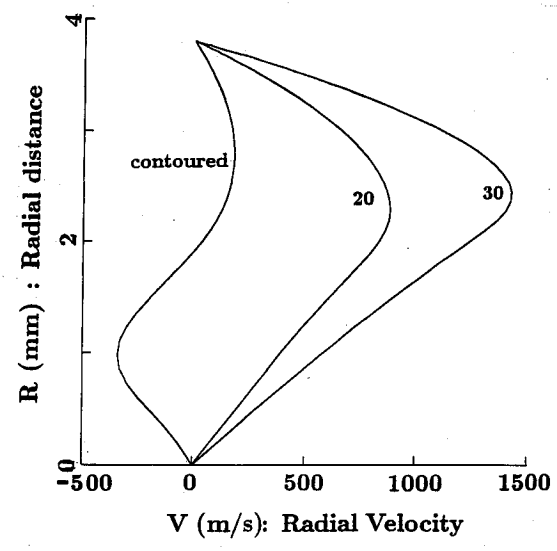

Fig. 8 Exit radial velocity profiles.

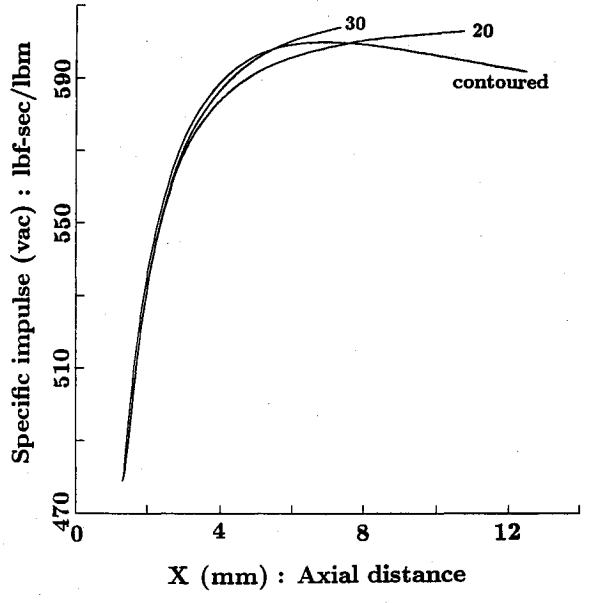

Fig. 9 Specific impulse variations with x.

Figure 9 shows the calculated vacuum specific impulse variations with axial distance. The vacuum specific impulse at a given axial station is defined as

$$I_{sp}(\text{vac}) = \left[2\pi\int_0^r (\rho u^2 + p) r \, dr\right] / \left[g 2\pi \int_0^{r_w} \rho u r \, dr\right] \quad (3)$$

where g is the standard acceleration of gravity (= 9.80665 m/s^2). The unit of the specific impulse is second which is the same as lb_f-s/lb_m.

As seen from this figure, the vacuum specific impulse of the contoured nozzle is the highest just downstream of the throat, but the lowest at the exit among those of the three nozzles. The highest specific impulse of the contoured nozzle just downstream of the throat can be explained by the fact that the increase in area ratio of the contoured nozzle is the highest just downstream of the throat. Even though the divergence loss of the 30-deg half-angle conical nozzle is larger than those of the other two nozzles due to its large exit angle, the vacuum specific impulse of 604 lb_f-s/lb_m, which is the highest among the three nozzles, is obtained for the 30-deg half-angle conical nozzle because of its shorter length, which results in a smaller viscous loss. The calculated vacuum specific impulses for the 20-deg half-angle conical and contoured nozzles are 603 and 592 lb_f-s/lb_m, respectively. For comparison, the vacuum specific impulse of a nozzle with an area ratio of 82, which is obtained by running the one-dimensional, inviscid code (CET85)[25] for the present chamber conditions, is 656 lb_f-s/lb_m.

Rothe Nozzle

The calculations are made for the Rothe nozzle with the chamber temperature of 300 K and the chamber pressure of 474 Pa. The throat Reynolds number at these chamber conditions is 270 and the computational grid is shown in Fig. 10. Figure 11 shows the Mach-number contour from the present calculations. As seen from this figure, the inviscid core is very small due to the significant viscous effect and the Mach number reaches about 4 on the centerline of the nozzle exit.

Figures 12 and 13 show the density variation along the centerline and the normalized density profile near the exit of the nozzle with the experimental data. As seen from Fig. 12, the calculated variation of the centerline density shows the same trend as that of the experimental data, but the centerline density from the present calculations is slightly higher than the experimental data. As shown in Fig. 13, the normalized density profile near the exit from the present calculations agrees reasonably well with the experimental data. The discrepancy between the present solutions and experimental data seems to be mainly due to the velocity slip at the wall and the exit boundary condition. Inside the Rothe nozzle, which is small in dimension and operated at an extremely low chamber pressure, the Knudsen number is much higher than the value for the continuum flow; thus, the flow is rarefied and there is a slip at the nozzle wall.[1]

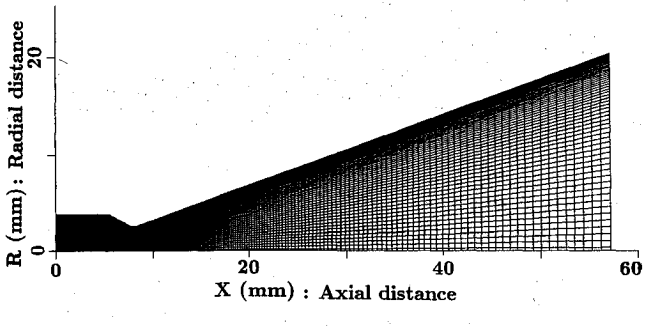

Fig. 10 Computational grid for the Rothe nozzle.

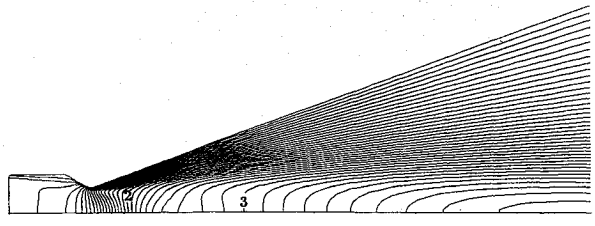

Fig. 11 Mach-number contour for the Rothe nozzle.

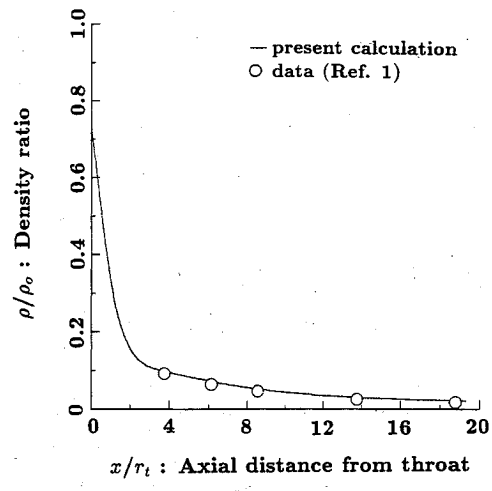

Fig. 12 Axial variation of centerline density in the Rothe nozzle.

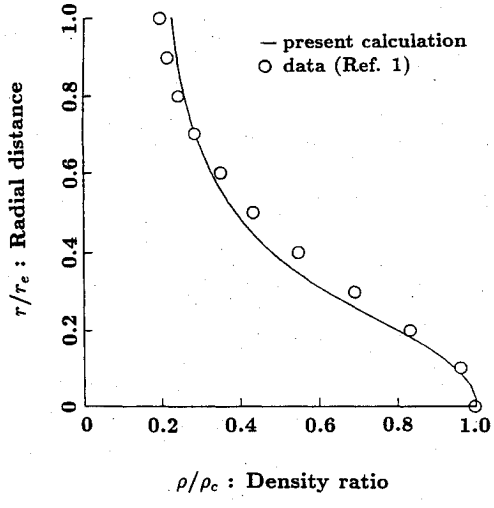

Fig. 13 Density profile near the exit of the Rothe nozzle.

Conclusions

Calculations are made for low-Reynolds-number resistojet nozzles using a full Navier-Stokes code. To study the effects of viscous and divergence losses on performance, flowfields and specific impulses of hydrogen resistojet nozzles with various lengths and shapes, such as 20-deg, 30-deg half-angle conical nozzles and a contoured nozzle whose wall contour is obtained from the Rao code, are calculated and compared with each other. The throat Reynolds number and area ratio of these resistojet nozzles are 1150 and 82, respectively. Even though the divergence loss of the 30-deg half-angle conical nozzle is the largest among those of the three nozzles due to its large exit angle, the highest vacuum specific impulse of 604 lb_f-s/lb_m is obtained for the 30-deg half-angle conical nozzle in which the viscous loss is the smallest due to its short length. The calculated vacuum specific impulses for the 20-deg half-angle conical and contoured nozzles are 603 and 592 lb_f-s/lb_m, respectively. Calculations are also made for the very low-Reynolds-number nitrogen flow in the nozzle whose throat Reynolds number and area ratio are 270 and 66 to validate the code, and the results agree reasonably well with the experimental data.

Acknowledgments

This work was supported by NASA Lewis Research Center under Contract NAS3-25266 with Robert M. Stubbs as the monitor. This work was performed using the computational resources of the NASA Lewis Research Center.

References

[1]Rothe, D. E., "Electron-Beam Studies of Viscous Flow in Supersonic Nozzle," *AIAA Journal*, Vol. 9, No. 5, 1971, pp. 804–811.

[2]Rae, W. J., "Some Numerical Results on Viscous Low-Density Nozzle Flows in the Slender-Channel Approximation," *AIAA Journal*, Vol. 9, No. 5, 1971, pp. 811–820.

[3]Driscoll, R. J., "Study of the Boundary Layers in Chemical Laser Nozzles," *AIAA Journal*, Vol. 14, No. 11, 1976, pp. 1571–1577.

[4]Whitfield, D. L., Lewis, J. W. L., and Williams, W. D., "Measurements in the Near Field of Supersonic Nozzles for Chemical Laser Systems," *AIAA Journal*, Vol. 12, No. 6, 1974, pp. 870–872.

[5]Greenberg, R. A., Schneiderman, A. M., Ahouse, D. R., and Parmentier, E. M., "Rapid Expansion Nozzles for Gas Dynamic Lasers," *AIAA Journal*, Vol. 10, No. 11, 1972, pp. 1494–1498.

[6]Whitfield, D. L., and Lewis, C. H., "Boundary-Layer Analysis of Low-Density Nozzles, Including Displacement, Slip, and Transverse Curvature," *Journal of Spacecraft and Rockets*, Vol. 7, No. 4, 1970, pp. 462–468.

[7]Whitfield, D. L., "Theoretical and Experimental Investigation of Boundary Layers in Low Density Hypersonic Axisymmetric Nozzles," Arnold Engineering Development Center, AEDC-TR-68-193, Arnold Air Force Base, TN, Sept. 1968.

[8]Murch, C. K., Broadwell, J. E., Silver, A. H., and Marcisz, T. J., "Low-Thrust Nozzle Performance," AIAA Paper 68-91, Jan. 1968.

[9]Brophy, J. R., Pivirotto, T. J., and King, D. Q.,"Investigation of Arcjet Nozzle Performance," AIAA Paper 85-2016, Sept. 1985.

[10]Grisnik, S. P., Smith, T. A., and Saltz, L. E., "Experimental Study of Low-Reynolds-Number Nozzles," NASA TM-89858, May 1987.

[11]Whalen, M. V., "Low-Reynolds-Number Nozzle Flow Study," NASA TM-100130, July 1987.

[12]Morren, W. E., Stuart, S. H., Hagg, T. W., and Sovey, J. S., "Performance Characterizations of an Engineering Model Multipropellant Resistojet," *Journal of Propulsion and Power*, Vol. 5, No. 2, 1989, pp. 197–203.

[13]Morren, W. E., Whalen, M. V., and Sovey, J. S., "Performance and Endurance Tests of a Laboratory Model Multipropellant Resistojet," *Journal of Propulsion and Power*, Vol. 6, No. 1, 1990, pp. 18–27.

[14]Rao, G. V. R., "Exhaust Nozzle Contour for Optimum Thrust ," *Jet Propulsion*, Vol. 28, June 1958, pp. 377–382.

[15]Nickerson, G. R., Coates, D. E., and Bartz, J. L., "Engineering Programming and Users Manual; Two-Dimensional Kinetic Reference Computer Program," NASA CR-152999, Dec. 1973.

[16]Shuen, J.-S., and Yoon, S., "Numerical Study of Chemically Reacting Flows Using a LU-SSOR Scheme," *AIAA Journal*, Vol. 27, No. 12, 1989, pp. 1752–1760.

[17]VanOverbeke, T. J., and Shuen, J.-S., "A Numerical Study of Chemically Reacting Flow in Nozzle, " NASA TM-102135, July 1989.

[18]Kim, S. C., and VanOverbeke, T. J., "Performance and Flow Calculations of Gaseous H_2/O_2 Thruster, " *Journal of Spacecraft and Rockets*, Vol. 28, No. 4, Aug. 1991, pp. 433–438.

[19]Kim, S. C., "Numerical Study of High-Area-Ratio H_2/O_2 Rocket Nozzles," AIAA Paper 91-2434, June 1991.

[20]Stubbs, R. M., Kim, S. C., and Benson, T. J., "Computational Fluid Dynamics Studies of Nuclear Rocket Performance," AIAA Paper 91-3577, Sept. 1991.

[21]Kim, S. C., and Stubbs, R. M., "Numerical Study of Low Pressure Nuclear Thermal Rockets," AIAA Paper 92-3815, July 1992.

[22]Yoon, S., and Jameson, A., "A LU-SSOR Scheme for the Euler and Navier-Stokes Equations," AIAA Paper 87-0600, Jan. 1987.

[23]Sovey, J. S., Penko, P. F., Grisnik, S. P., and Whalen, M. V.,"Vacuum Chamber Pressure Effects on Thrust Measurements of Low-Reynolds-Number Nozzles," NASA TM-86955, April 1985.

[24]Manzella, D. H., Penko, P. F., De Witt, K. J., and Keith, T. G., Jr., "Effect of Ambient Pressure on the Performance of a Resistojet," *Journal of Propulsion and Power*, Vol. 5, No. 4, 1989, pp. 452–456.

[25]Gordon, S., and McBride, B. J., "Computer Program for Calculation of Complex Chemical Equilibrium Compositions, Rocket Performance, Incident and Reflected Shocks, and Chapman-Jouguet Detonations," NASA SP-273, March 1976.

James A. Martin
Associate Editor